



Semilagrangian schemes applied to moving boundary problems for the BGK model of rarefied gas dynamics

Giovanni Russo, Francis Filbet

► To cite this version:

Giovanni Russo, Francis Filbet. Semilagrangian schemes applied to moving boundary problems for the BGK model of rarefied gas dynamics. *Kinetic and Related Models*, 2009, 2 (1), pp.231-250. 10.3934/krm.2009.2.231 . hal-00659672

HAL Id: hal-00659672

<https://hal.science/hal-00659672>

Submitted on 13 Jan 2012

HAL is a multi-disciplinary open access archive for the deposit and dissemination of scientific research documents, whether they are published or not. The documents may come from teaching and research institutions in France or abroad, or from public or private research centers.

L'archive ouverte pluridisciplinaire **HAL**, est destinée au dépôt et à la diffusion de documents scientifiques de niveau recherche, publiés ou non, émanant des établissements d'enseignement et de recherche français ou étrangers, des laboratoires publics ou privés.

SEMILAGRANGIAN SCHEMES APPLIED TO MOVING BOUNDARY PROBLEMS FOR THE BGK MODEL OF RAREFIED GAS DYNAMICS

GIOVANNI RUSSO

Dipartimento di Matematica e Informatica
Università di Catania
Viale Andrea Doria 6, 95125 Catania, Italy

FRANCIS FILBET

Université de Lyon, U11, INSAL, ECL, CNRS
UMR5208, Institut Camille Jordan
43 boulevard 11 novembre 1918, F-69622 Villeurbanne cedex, France

ABSTRACT. In this paper we present a new semilagrangian scheme for the numerical solution of the BGK model of rarefied gas dynamics, in a domain with moving boundaries, in view of applications to Micro Electro Mechanical Systems (MEMS). The source term is treated implicitly, which makes the scheme Asymptotic Preserving in the limit of small Knudsen number. Because of its Lagrangian nature, no stability restriction is posed on the CFL number, which is determined only by accuracy requirements. The method is tested on a one dimensional piston problem. The solution for small Knudsen number is compared with the results obtained by the numerical solution of the Euler equation of gas dynamics.

1. Introduction. Microscopic description of a gas, neglecting quantum effect, could be obtained by solving the equation of motion for a collection of a large number N_g of molecules. For most cases of practical relevance, such a task would require an enormous amount of computer power (at standard condition of temperature and pressure in a cubic millimeter there are about 3×10^{16} molecules), furthermore, such an amount of information, even if available, would be extraordinarily redundant.

Rarefied gas flow can be treated at a mesoscopic level by a kinetic description, in terms of a distribution function $f(t, x, v)$ which gives the probability density of finding a gas molecule with velocity v at position x at time t . At this level, when short-range binary collisions among the molecules are the dominant effect, the evolution of the distribution function is governed by the Boltzmann equation, a non linear integrodifferential equation [11]. This description is satisfying when the number of molecules is large enough to justify a statistical approach. If the mean free path of molecules is much smaller than the macroscopic typical size of the system, then even a kinetic description is redundant, and one can safely obtain

2000 Mathematics Subject Classification. Primary: 76P05, 76M20; Secondary: 82C80.

Key words and phrases. Rarefied gas flows, Boltzmann equation, Lagrangian methods, Numerical methods for time dependent statistical mechanics.

This paper is dedicated to the memory of Angelo Marcello Anile, advisor, mentor and friend of the first author.

accurate predictions by using a continuum description of the gas, in terms of Euler or Navier-Stokes equations.

Rarefied regimes may appear when considering the motion of objects in the outer atmosphere, where the mean free path may be comparable or even larger than man-powered vehicles (at 100 Km the mean free path is about 1 m, and then it rapidly increases with altitude [1]). For this reason the Boltzmann equation has been widely studied by aerospace engineers.

There are, however, other contexts in which rarefied gas dynamics has to be used even at standard temperature and pressure; for example, when considering flow of gas in micro channels, the length of the characteristic size of the device may be comparable with the mean free path. A very important case is represented by rarefied gas flows in MEMS [21], Micro-Electro-Mechanical-Systems which are built by photolithographic techniques similar to the integrated circuits of microelectronics. A large class of devices, including accelerometers, micro pumps, micro engines, and so on can be built with this technique. The advantages of MEMS with respect to their larger traditional counterparts, is the small size, the reliability and robustness, and the low cost for mass production.

Some MEMS, such as accelerometers, are composed by several elements, which consist by a part, the "stator", fixed to the substrate, and a suspended part, the "shuttle", which is free to oscillate at moderate frequency in a certain specified direction. The oscillations induce a change in the capacitance of the element, which can be detected, and used to measure the acceleration of the device in the direction of the degree of freedom.

The behavior of MEMS involves several interacting physical effects, including structural dynamics, electrical properties and gas dynamics, and full modeling is really a multi physics problem.

An important aspect of the dynamics is due to the interaction of the moving part with the gas inside the device. Because of the small size of the channels, the mean free path of the gas can be comparable to the width of the channel. Under such conditions, Navier-Stokes equations are not adequate to model gas flow, and one has to resort to a kinetic description.

In the work [20] the authors treat the gas flow in one element of an accelerometer by means of the BGK model or rarefied gas dynamics (see next section), which is a relaxation time approximation of the Boltzmann equation, and provides a crude description of the effect of the collisions. In spite of the simplification, they are able to obtain results in very good agreement with experimental measurements of the damping effect of the gas.

In that paper, the authors use a quasi-static approximation: the flow field of the gas is a steady state computation, in which the motion of the moving part is taken into account by assigning suitable boundary conditions. For moderate accelerations this approach is justified by the consideration that the speed of the moving element is much smaller than thermal speed of the gas, and therefore in a very short time, the gas approaches steady state, while the shuttle barely moved.

When the speed of the element is not negligible with respect to thermal velocity, then the motion of the shuttle, and consequently the time dependence of the domain in which the fluid flows, has to be taken into account.

This consideration motivates the research of effective ways to solve kinetic equations in a time dependent domain.

The numerical solution of the Boltzmann equation constitutes a challenge, because of the high dimensionality of the problem, and because of the difficulty in accurately and efficiently computing the quadratic collisional term. Several numerical methods have been developed for this purpose. A review of the literature on most commonly used deterministic and stochastic methods can be found, for example, in the lecture notes [27].

Stochastic methods, such as Direct Simulation Monte Carlo (DSMC) [7], have been widely used because of their efficiency, and their ability to deal with large deviation from equilibrium. Such methods, however, are not suitable for low Mach number flow, because of the inherent statistical noise, which tends to mask small deviation from thermodynamical equilibrium. Furthermore, DSMC is quite effective for stationary problems, where time averages can be taken to accumulate statistics, and reduce fluctuations. Here we are mainly interested in low Mach number, time dependent problems.

In such conditions, deterministic methods are probably more effective. Although there are relatively efficient and accurate deterministic methods for the numerical approximation of the Boltzmann collisional operator, such as spectral methods based on the Fourier representation (see [29, 18] for space homogeneous problems, and [19] for spatially non homogeneous problems), here the main emphasis is on the treatment of moving boundaries, therefore we shall use the simple BGK model, which is able to capture some of the essential features of the flow. Furthermore, thanks to the simple structure, it is possible to construct a numerical scheme that is Asymptotic Preserving, i.e. that becomes a consistent scheme for the fluid dynamic limit (see [14, 23] for AP schemes in the context of kinetic equations).

The plan of the paper is the following. In the next section we briefly recall the BGK model, and relative fluid dynamic limit. In Section 3 we describe the semi-implicit Lagrangian method for the BGK model. Section 4 is devoted to the description of the boundary conditions for the piston problem. The last section presents numerical tests for various values of the Knudsen number. A comparison with the solution of the piston problem for the Euler equations of gas dynamics is also performed. Finally, we draw conclusions and address future work.

2. The BGK model. The BGK model was introduced by Bhatnagar, Gross and Krook [6] as a simplification of the Boltzmann equation, where the collisions are modeled by a relaxation of the distribution function $f(t, x, v)$ towards the Maxwellian equilibrium. It consists of the following initial boundary value problem

$$\begin{aligned} \frac{\partial f}{\partial t} + v \cdot \nabla_x f &= \frac{1}{\tau} (M[f] - f) \\ f(0, x, v) &= f_0(x, v) \quad t \geq 0, \quad x \in \mathbb{R}^{d_x}, v \in \mathbb{R}^{d_v}. \end{aligned} \quad (1)$$

In the equation (1) $M[f]$ is the Maxwellian obtained by the moment of the distribution function f ,

$$M[f] = \frac{\rho}{(2\pi RT)^{d_v/2}} \exp\left(-\frac{|v - u|^2}{2RT}\right). \quad (2)$$

In this formulation d_x and d_v denote the dimensions of the physical and velocity space respectively, while ρ , u and T denote the macroscopic fields, namely: density, velocity and temperature. R is the universal gas constant divided by the molecular mass of the gas. Once the problem is solved, the distribution function is known

and the macroscopic fields are obtained as moments of f . Let $\phi(v) = (1, v, 1/2|v|^2)$ denote the vector of the collision invariants. Then the moments are given by

$$(\rho, \rho u, E) = \langle f \phi(v) \rangle \equiv \int_{\mathbb{R}^{d_v}} \phi(v) f(t, x, v) dv$$

The quantity $E(x, t)$ is the total energy density and it is related to the the temperature by the internal energy $e(x, t)$

$$e(x, t) = \frac{d_v}{2} RT(x, t), \quad \rho e = E - \frac{1}{2} \rho u^2.$$

2.1. Conservation laws. By the definition of moments of the distribution function, one obtains the following conservation laws for the mass density, momentum density, and energy density

$$\begin{aligned} \frac{\partial \langle f \rangle}{\partial t} + \nabla_x \cdot \langle f v \rangle &= 0, \\ \frac{\partial \langle f v \rangle}{\partial t} + \nabla_x \cdot \langle v \otimes v f \rangle &= 0, \\ \frac{\partial \langle \frac{1}{2} |v|^2 f \rangle}{\partial t} + \nabla_x \cdot \langle \frac{1}{2} |v|^2 f v \rangle &= 0. \end{aligned} \tag{3}$$

Notice that the above system for the moments is in general not closed, because the number of unknowns is larger than the number of equations.

Generally BGK models are implemented using $d_v = 3$, this means that the system is a mono atomic gas with three translational degrees of freedom. Mathematical models of gas with only $d_v = 2$ or $d_v = 1$ degrees of freedom are also possible.

In this paper we shall deal with the case $d_v = 1$, which simplifies the numerical computations, without affecting the qualitative results. The same model has been used in [14].

The collision frequency $\nu \equiv \tau^{-1}$ for the BGK model may be a function of the density ρ (generally linear) and temperature. Several models are discussed in [3].

All the computations in the present paper are performed by assuming that τ is constant. If we write the equation in non dimensional form, then τ becomes the Knudsen number, i.e. the ratio between the collision time and the macroscopic time scale typical of the system.

2.2. Fluid dynamic limit. In the fluid dynamic limit, i.e. as $\tau \rightarrow 0$, the distribution function will converge to a local Maxwellian, and the system (3) becomes a closed system for the $2 + d_x$ moments. The conserved quantities satisfy the classical Euler equations of gas dynamics for a mono atomic gas:

$$\begin{aligned} \frac{\partial \rho}{\partial t} + \sum_{j=1}^{d_x} \frac{\partial \rho u_j}{\partial x_j} &= 0, \\ \frac{\partial \rho u_i}{\partial t} + \sum_{j=1}^{d_x} \frac{\partial}{\partial x_j} (\rho u_i u_j + p \delta_{ij}) &= 0, \\ \frac{\partial E}{\partial t} + \sum_{i=1}^{d_x} \frac{\partial}{\partial x_i} (u_i (E + p)) &= 0. \end{aligned} \tag{4}$$

Eq. (4) constitutes a system of $2 + d_x$ equations in $3 + d_x$ unknowns. The pressure is related to the internal energy by the constitutive relation for a polytropic gas

$$p = (\gamma - 1)(E - \frac{1}{2}\rho|u|^2), \quad (5)$$

where the polytropic constant $\gamma = (d_v + 2)/d_v$ represents the ratio between specific heat at constant pressure and at constant volume.

For small but non zero values of the Knudsen number, the evolution equation for the moments can be derived by the so-called Chapman-Enskog procedure [12], applied to the BGK equation. This approach, however, does not give the correct value of the Prandtl number of the Navier-Stokes equations: because there is only one fitting parameter (the relaxation time), one can only match either the thermal conductivity or the fluid viscosity. The proper value of the Prandtl number can be restored by making use of the so called elliptic BGK-model (see, for example, [22, 8, 4]).

3. Description of the method. We describe the numerical method in the simple case of one dimension in space and velocity. First let us assume that the integration domain in space is $[0, L]$, with a fixed L . The initial-boundary value problem can be written as

$$\begin{aligned} \frac{\partial f}{\partial t} + v \frac{\partial f}{\partial x} &= \frac{1}{\tau}(M[f] - f), \\ f(t, x, v) &= f_0(x, v) \end{aligned} \quad (6)$$

where $v \in \mathbb{R}$, $x \in [0, L]$, and $t > 0$. Different boundary conditions can be prescribed at $x = 0$ and $x = L$.

Suppose we want to integrate the equation up to a fixed time $t = t_f$. For simplicity we assume constant time step $\Delta t = t_f/N_t$ and uniform grid in physical and velocity space, with mesh spacing Δx and Δv , respectively, and denote the grid points by $t_n = n\Delta t$, $x_i = i\Delta x$, $i = 0, \dots, N_x$, $v_j = j\Delta v$, $j = -N_v, \dots, N_v$, where $N_x + 1$ and $2N_v + 1$ are the number of grid nodes in space and velocity, respectively. We assume that the distribution function is negligible for $|v| > v_{\max} = N_v\Delta v$. We denote by $f_j(t, x)$ a numerical approximation of the function $f(t, x, v_j)$. The evolution equation for $f_j(t, x)$ along the characteristics between time step n and time step $n + 1$ is obtained by writing (6) in characteristic form for $f_j(t, x)$

$$\begin{aligned} \frac{df_j}{dt} &= \frac{1}{\tau}(M_j[f] - f_j), \\ \frac{dx}{dt} &= v_j, \\ x(t_n) &= \bar{x}, \quad f_j(t_n) = f_j^n(\bar{x}), \quad t \in [t_n, t_{n+1}], \end{aligned} \quad (7)$$

Here $M_j(t, x)$ denotes the local Maxwellian with the same moments of the function $f(t, x, \cdot)$ evaluated at velocity v_j .

Let f_{ij}^n denote the approximation of the solution $f(t_n, x_i, v_j)$ of the problem (6) at time t_n in each spatial and velocity node, and assume that it is given.

A first order scheme is obtained by discretizing Eq.(7) in time. Since we are interested in a scheme which is stable even for small relaxation time, we discretize Eq. (7) by implicit Euler scheme

$$\begin{aligned} f_{ij}^{n+1} &= \tilde{f}_{ij}^n + \frac{\Delta t}{\tau}(M_{ij}^{n+1} - f_{ij}^{n+1}), \\ x_i &= \tilde{x}_{ij} + v_j\Delta t, \quad i = 0, \dots, N_x, \quad j = -N_v, \dots, N_v. \end{aligned} \quad (8)$$

The scheme is illustrated in Figure 1.

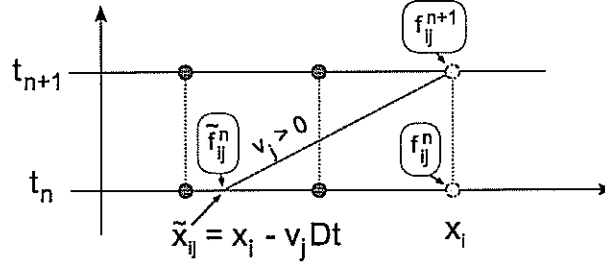


FIGURE 1. Space-time grid for the computation of f_{ij}^{n+1}

The value of the function \tilde{f}_{ij}^n is reconstructed at position $\tilde{x}_{ij} = x_i - v_j \Delta t$ by a suitable high order reconstruction. In particular, here we use a piecewise cubic polynomial, which is obtained by Hermite interpolation in each interval $[x_i, x_{i+1}]$. The first derivatives of the function at location x_i , $(\partial f_j / \partial x)_{x_i}$, are computed by second order central difference (see Figure 2),

$$\left(\frac{\partial f_j}{\partial x} \right)_{x_i} \approx \frac{f_{i+1,j} - f_{i-1,j}}{2\Delta x}.$$

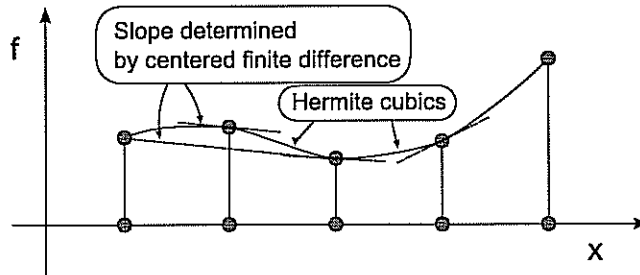


FIGURE 2. Piecewise Hermite interpolation for the reconstruction of the distribution function off the grid

The reconstruction is linear, without limiters. This guarantees that the scheme is conservative [17].

Other reconstructions are possible. For example, Carrillo and Vecil [10] use WENO reconstruction, when applying semilagrangian schemes to Vlasov-like equations, while Santagati used high order pointwise WENO [9], and high order Runge-Kutta schemes, to obtain high order accuracy in time [31].

Remark 1. We observe that if $\Delta x = \Delta v \Delta t$ then $\tilde{x}_{ij} = x_i - v_j \Delta t = x_i - j \Delta x = x_{i-j}$, therefore the foot of the characteristics is a grid point, and no reconstruction is required. In such a case, the scheme becomes a lattice Boltzmann method (LBM, see, for example, [13]), although LBM are in general used to model fluid dynamic effect using a limited number of velocities, rather than as a numerical tool for kinetic

equations, as we do here. LBM have been widely used because they can be efficiently coded, are easily parallelizable, and allow treatment of complex geometries. If the foot of the characteristics is not a grid point, then the schemes are sometimes referred to as *off-lattice Boltzmann* schemes [5].

Other characteristic-based methods have been used in the literature for the numerical solution of the BGK model. For example, in [5], the authors use a characteristic method based on the approach used in [32]. Their scheme, however does not use high order reconstruction, and suffers from stability restriction of CFL type.

3.1. Implicit calculation. The implicit term can be explicitly computed making use of the following observation. By definition, the Maxwellian $M_{i,\cdot}^{n+1}$ and the function $f_{i,\cdot}^{n+1}$ have the same conservative moments ρ_i^{n+1} , $(\rho u)_i^{n+1}$, E_i^{n+1} . Under the assumption that the distribution function is smooth, and that the energy outside the computational domain in velocity is negligible, the moments are approximated with spectral accuracy by replacing the integral in velocity by summation.

Let us multiply Eq. (8) by $1, v, |v|^2$ and sum over the velocities. Because $M_{i,\cdot}^{n+1}$ and $f_{i,\cdot}^{n+1}$ have the same moments, one obtains

$$\rho_i^{n+1} = \sum_j \bar{f}_{ij}^n, \quad (\rho u)_i^{n+1} = \sum_j v_j \bar{f}_{ij}^n, \quad E_i^{n+1} = \frac{1}{2} \sum_j |v_j|^2 \bar{f}_{ij}^n. \quad (9)$$

Once the moments have been computed, the Maxwellian can be calculated from the moments, and the density function can be explicitly computed as

$$f_{ij}^{n+1} = \frac{\tau \bar{f}_{ij}^n + \Delta t M_{ij}^{n+1}}{\tau + \Delta t}. \quad (10)$$

Notice that as $\tau \rightarrow 0$ the distribution function f_{ij}^{n+1} is projected onto the Maxwellian. Furthermore, in this limit the whole scheme becomes a relaxation scheme for the Euler equations. We say that the scheme is *Asymptotic Preserving*. This term was introduced by Shi Jin in the context of numerical method for kinetic equations that are able to capture the fluid dynamic limit [23], and by Axel Klar [24], in the context of kinetic equations close to the low Mach number limit, although the concept was already present in the paper by Coron and Perthame [14].

In the context of numerical methods for systems of ordinary differential equations, the property of being AP is essentially the capability of a method, applied to a stiff system, to become a consistent discretization of the underlying limit system of differential-algebraic equations, and it is strongly related to L-stability property of the method. A vast literature is available for numerical methods with such a property. In the context of hyperbolic equations with relaxation, high order Implicit-Explicit schemes that are Asymptotic Preserving have been derived (see, for example, [27]). A new methodology has recently been introduced for the development of Asymptotic Preserving schemes in several contexts, which is based on the reformulation of the singularly perturbed problem into an equivalent problem, in which the singularity has been removed. See for example the paper [15] for an application to the Euler-Poisson equation near the quasi-neutral limit.

Remark 2. We remark here that the moments computed by the discrete summation in Eq.(9) are not exactly equal to the moments computed integrating the continuous Gaussian (2). This may lead to a small inconsistency of the method. To overcome this problem, Mieussens introduced a discrete Maxwellian that depends also on three

parameters, related to the moments [25]; the determination of such parameters requires the solution of a non linear system. However, if the solution is regular, the discrepancy between the moments computed by the standard Gaussian and the discrete distribution used by Mieussens is very small, because of the spectral accuracy of the quadrature formulas. Some comparison obtained by using the two approaches is shown in the paper by Pieraccini and Puppo [30].

4. The piston problem. In view of the application to MEMS, in this section we consider a simple problem in a domain with moving boundary. The system consists in a gas inside a one dimensional slab, which is driven by a moving piston (see Figure 3). On the left boundary of the domain there is a fixed wall (the origin of our coordinate system), at the right end there is a piston, whose position is an assigned function of time $x_p : t \in \mathbb{R} \rightarrow x_p(t) \in [0, L]$. We assume that the gas inside the slab is governed by the BGK equation. The system is discretized on a uniform grid in the computational domain $[0, L]$ by $N_x + 1$ grid points of coordinates $x_i = ih, i = 0, \dots, N_x, h = L/N_x$. As the piston moves, the domain occupied by the gas changes, while the position of the grid points remains fixed. As a consequence, only a certain number $N_x(t)$ of grid points is actually used (*active points*) while other points lie outside of the domain (*ghost points*).

The number of equations to be solved changes with time. We choose the time step in such a way that the piston can move by at most one grid point in one step, i.e.

$$\max_{0 \leq t \leq t_f} |u_p(t)| \Delta x < \Delta t,$$

where $u_p(t) \equiv \dot{x}_p(t)$ is the assigned piston velocity. Let us define by $N_n = N_x(t_n)$ the number of active grid points at time step n .

There are only three possibilities: i) $N_{n+1} = N_n$, ii) $N_{n+1} = N_n + 1$, iii) $N_{n+1} = N_n - 1$. Figure 4 illustrates the first two cases.

At each time step, the number of unknowns to be determined is given by $(N_{n+1} + 1)(2N_v + 1)$.

Different boundary conditions may be assigned to the boundary. Here we consider two extreme conditions, namely specular reflection and diffusive boundary conditions. It is clear that a convex combination of these two conditions is possible (Maxwell boundary conditions) at either boundary (piston or wall).

4.1. Specular reflection. The conditions for specular reflection are the following. At the wall, at each time t , the distribution function, for positive velocities, is given by

$$f(t, 0, v) = f(t, 0, -v).$$

This condition is equivalent to replace the wall by a gas with a specularly symmetric distribution for $x < 0$. With this in mind, we can easily convert the boundary conditions into initial value conditions for the *ghost* points. For example, this is obtained by defining the ghost values of f_{ij} for $i < 0$ and $v_j > 0$, as

$$f_{-i,j}^n = f_{i,-j}^n, \quad i \leq 0, j > 0,$$

keeping in mind that $v_j = j\Delta v$. In this way the problem on the left boundary is converted into an initial value problem, and the same procedure used for the points well inside the domain can be used for the points near the boundary. The number of ghost points that needs to be set is given by $N_{GL} = \lfloor V_{\max} \Delta t / \Delta x \rfloor + 1$, where $\lfloor \cdot \rfloor$ denotes the integer part.

A similar condition can be used to treat reflecting boundary conditions near the piston:

$$f(t, x_p, v) = f(t, x_p, v^*), \quad v^* = 2u_p - v.$$

As in the case of the wall, this condition is not of immediate application, because it requires the knowledge of the function at the piston, for arbitrary time $t \in [t_n, t_{n+1}]$. We convert the condition into an initial value for the ghost point using the following argument. We approximate the motion of the piston by a piecewise linear function of time, i.e. we assume that in time interval $[t_n, t_{n+1}]$ the velocity of the piston is unchanged. Then the value of the density function $f(t_n, \bar{x}_{ij}, v_j)$, at the foot of the characteristics corresponding to the velocity $v_j < u_p$, is set to $f^n(x^*, v^*)$, where $x_{ij} + x^* = 2x_p(t_n)$ and $v_j + v^* = 2u_p(t_n)$ (see Figure 5). The simplest way to implement such condition is to precompute the values of the distribution function at ghost points $x_i > x_p(t_n)$, for $v_j < u_p$, as $f^n(x_i, v_j) = f^n(x^*, v^*)$, with $x_i + x^* = 2x_p(t_n)$ and $v_j + v^* = 2u_p(t_n)$, and then use the standard piecewise Hermite interpolation from grid points (active or ghost) at time level t_n . In general point (x^*, v^*) is not on a grid in phase space, therefore interpolation in x and v has to be used. In some cases, point (x^*, v^*) is in a cell whose values of the function is known at the vertices, and bilinear interpolation can be used. In other cases, the function at the vertices is itself not known, and an iterative procedure has to be used. This procedure is illustrated in Figure 6. Note that the use of bilinear interpolation degrades the accuracy near the boundary.

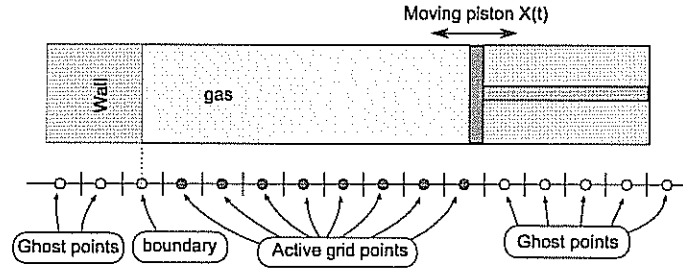


FIGURE 3. Setup of the piston problem. The equations are solved for the values of the distribution function in the active grid points. The values outside of the computational domain (*ghost points*) are computed by making use of the boundary conditions

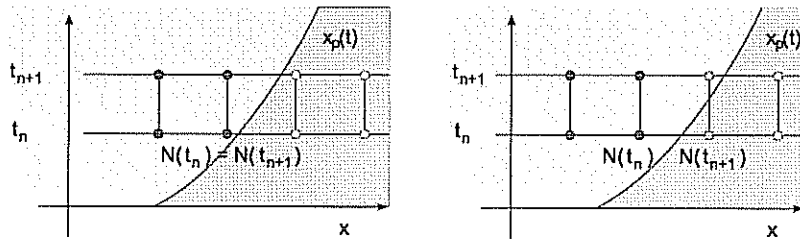


FIGURE 4. The number of active grid points depends on time. Left: $N_x(t_{n+1}) = N_x(t_n)$; right: $N_x(t_{n+1}) = N_x(t_n) + 1$

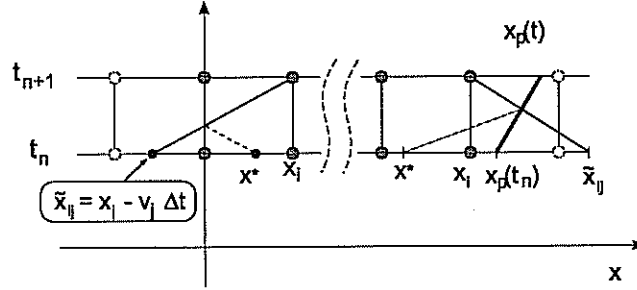


FIGURE 5. Definition of the specular boundary conditions at the wall (left) and at the piston (right)

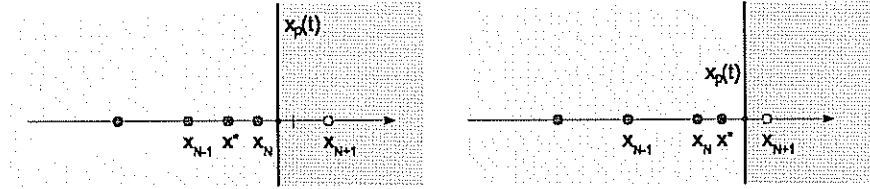


FIGURE 6. Definition of the ghost values. Left: $x_p < (x_{N+1} + x_N)/2$. Interpolation is possible without iteration; right: $x_p > (x_{N+1} + x_N)/2$. Iteration is required to interpolate

4.2. Diffusive boundary conditions. Diffusive boundary conditions are implemented as follows. Let us assume that the velocity of the piston is piecewise constant in time. There are three cases, according to whether $N_{n+1} = N_n$, $N_{n+1} = N_n + 1$, and $N_{n+1} = N_n - 1$. Since all three cases will be treated in a similar way, in Figure 7 we illustrate just the first one.

Let us denote by the subscript “ p ” the quantities that refer to the piston. The density function at the piston, at time $n+1$ will be computed as follows: for velocities $v_j > u_p$ it is computed from the evolution equation. For velocities $v_j < u_p$ it is a Maxwellian, with average velocity equal to the piston velocity, and with a density such that the net mass flux across the piston is zero.

For velocities smaller than the piston velocity (i.e. for characteristic entering the domain), one has

$$M_{pj}^{n+1} = \frac{\rho_p}{\sqrt{2\pi RT_p}} \exp\left(-\frac{(v_j - u_p)^2}{2RT_p}\right), \quad v_j < u_p$$

where T_p denotes the piston temperature. The density ρ_p is determined by imposing that

$$\sum_{v_j < u_p} M_{pj}^{n+1}(v_j - u_p) + \sum_{v_j > u_p} f_{pj}^{n+1}(v_j - u_p) = 0.$$

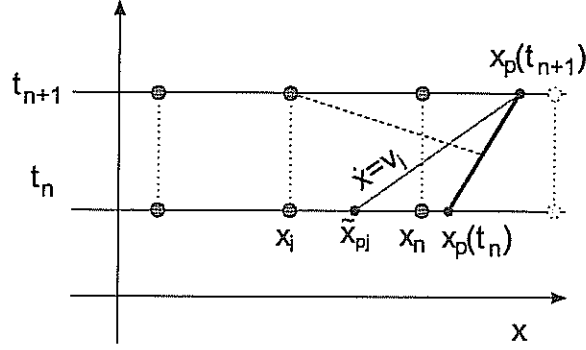


FIGURE 7. Diffusive boundary conditions at the piston. The value of the function at point $(t_{n+1}, x_p(t_{n+1}))$ for $v_j > u_p$ is computed from the evolution equation. The density ρ_p^{n+1} of the Maxwellian emitting from the wall at the same point is computed by imposing conservation of mass. The value of the function for characteristic entering the domain (dashed line) are computed by linear interpolation.

The Maxwellian M_{pj}^{n+1} , for $v_j > u_p$ is computed using the evolution equation for f . We trace the characteristics $v_j > u_p$, and, for those, we have the equation

$$f_{pj}^{n+1} = \tilde{f}_{pj}^n + \frac{\Delta t}{\tau} (M_{pj}^{n+1} - f_{pj}^{n+1}), \quad \forall v_j > u_p. \quad (11)$$

Then we multiply by the collision invariants, and obtain

$$\sum_j \phi_j M_{pj}^{n+1} = \sum_j \phi_j f_{pj}^{n+1}. \quad (12)$$

Observing that

$$f_{pj}^{n+1} = M_{pj}^{n+1} \quad \forall v_j \leq u_p,$$

equality (12) is valid also if we sum only over $v_j > u_p$, therefore we obtain

$$\sum_{v_j > u_p} \phi_j M_{pj}^{n+1} = \sum_{v_j > u_p} \phi_j f_{pj}^{n+1} = \sum_{v_j > u_p} \phi_j \tilde{f}_{pj}^n.$$

Once the three parameters that identify the fraction of Maxwellian for $v_j > u_p$ are determined, the distribution function can be computed from (11).

Once the distribution function is known at $x_p(t_n)$ and $x_p(t_{n+1})$, one can compute any needed value at the intersection between the characteristic corresponding to velocity $v_j < u_p$ ending at location $x_i < x_p$ for $t = t_{n+1}$ (see dashed line in Figure 7) by linear interpolation. If a characteristic reaching point x_i starts in the interval $[x_{N_n}, x_p(t_n)]$, then one can use linear interpolation between such points.

The use of linear interpolation near the boundary will decrease the accuracy of the scheme to first order near the boundary. Higher order approximation will be subject of future investigation.

Remark 3. The procedure just described is not exactly conservative, because the density corresponding to the ingoing Maxwellian particles are computed at the end points $(t_n, x_p(t_n))$ and $(t_{n+1}, x_p(t_{n+1}))$, and linear interpolation is used for

the characteristics entering the domain. Exact conservation could be restored by imposing that the (exact) total discrete next flux across the piston is zero.

5. Numerical tests. For our numerical tests we consider a slab of total length $L = 20$. The piston is located at the left boundary of the domain, while on the right edge there is a fixed wall. In all our tests we choose specular reflection both at the wall and at the piston. In this way, we shall be able to compare the solution of the BGK model with the numerical solution of the Euler equation of gas dynamics.

We solve the following problem

$$\begin{aligned} \frac{\partial f}{\partial t} + v \frac{\partial f}{\partial x} &= \frac{1}{\tau} (M[f] - f), \quad x \in (x_p(t), L), v \in \mathbb{R}, t \geq 0, \\ f(t, x_p(t), v) &= f(t, x_p(t), v^*), \quad v \in \mathbb{R} \\ f(t, L, v) &= f(t, L, -v), \quad v \in \mathbb{R} \end{aligned} \quad (13)$$

with $v + v^* = 2u_p(t)$.

We have computed a numerical solution for different Knudsen numbers, from rarefied regime up to the fluid limit. The solution in the hydrodynamic limit is also compared with the numerical solution of Euler system computed in Lagrangian coordinates using a large number of points, as described later in this section.

In a first set of tests we consider a piston that sets in motion with zero velocity. The initial data is given by $(\rho, u, T) = (1, 0, 1)$ for $x_p(0) \leq x \leq L$ and is a Maxwellian distribution in velocity, where the piston has an initial position $x_p(0) = 1$ and a velocity $u_p(t) = 0.25 \sin(t)$. All computations have been performed with $v_{\max} = 16$.

In Fig. 8, 9 we plot the results obtained in the rarefied regime ($\tau = 10^0, 10^{-1}$) using the semi-Lagrangian scheme. The scheme is used with 301 points in x and the size of the velocity grid is 301 points with a time step $\Delta t = 10^{-3}$.

We also give the result of the computations close to the Euler limit with $\tau = 10^{-3}$ using 601 space and velocity cells for the semi-Lagrangian method and the time step is $\Delta t = 10^{-3}$ (Fig. 10).

The small amplitude sinusoidal piston motion induces a wave that propagates into the domain. As the relaxation time is decreased, the singularity in the profile becomes sharper.

For the same test problem, we compute the evolution of the pressure at the piston and at the wall, for a time larger than the travel time of the wave in the slab. The results of the computation is reported in Figure 11, where a comparison is performed with an accurate solution of the Euler equations of gas dynamics, obtained with 1600 grid points. The detail about the gas dynamics calculations are explained in the next subsections. The agreement between the pressure profiles is quite remarkable.

As a second test, we consider a problem in which the piston starts with a finite velocity. The initial condition for the gas is the same as in the previous case, with $x_p(0) = 1.5$, and $u_p(t) = \cos(t)$.

A shock wave is created by the motion of the piston and propagates inside the gas. The profiles of density, gas velocity, and temperature are illustrated in Figure 12, at time $t = 5$, before the perturbation hits the wall. The continuous line represents the solution of the BGK model with reflecting BC, obtained with the method illustrated above, while the dashed line represents the solution of the Euler equation for a polytropic gas with $\gamma = 3$, obtained with 2000 space grid points. The agreement between the two solutions is remarkable, if we consider that they have

been obtained by solving different problems with completely different approaches. The discrepancy is mainly attributed to the finite relaxation time $\tau = 0.001$, and to the low space resolution in the solution of the BGK equation, for which we used a number of points that varies from a minimum of 263 to a maximum of 293, and a number of $2N_v + 1 = 301$ grid points in velocity space.

5.1. Piston problem for the Euler equations in Lagrangian form. A simple way to treat the one dimensional piston problem for the Euler equations is to write them in Lagrangian coordinates. Since the piston is a material point, the problem is defined in a fixed domain.

By introducing the Lagrangian coordinate ξ given by

$$\xi = \int_0^x \rho(z, t) dz ,$$

the Euler equations (4), written in one space dimension in Lagrangian form are

$$\frac{DV}{Dt} - \frac{\partial u}{\partial \xi} = 0, \quad \frac{Du}{Dt} + \frac{\partial u}{\partial \xi} = 0, \quad \frac{D\mathcal{E}}{Dt} + \frac{\partial(u p)}{\partial \xi} = 0,$$

where the time derivative is the Lagrangian derivative

$$D/Dt = \partial/\partial t + u\partial/\partial x ,$$

and the new field variables are the specific volume $V(\xi, t) = 1/\rho$, the gas velocity u , energy density per unit mass, $\mathcal{E} = E/\rho$, and the equation of state (5) becomes

$$p = (\gamma - 1) \left(\mathcal{E} - \frac{1}{2} u^2 \right) / V . \quad (14)$$

Note that the total mass

$$\xi_{\max} = \int_0^{x_p(t)} \rho(z, t) dz$$

is constant. The inverse transformation of coordinates is given by

$$x = \int_0^\xi V(z, t) dz . \quad (15)$$

The interval $0 \leq \xi \leq \xi_{\max}$ will be our “computational domain” in which we have a fixed uniform grid with $\xi_j = (j - 1/2)\Delta\xi$, $j = 1, 2, \dots, J$, denoting the center of j -th cell, and $\Delta\xi = \xi_{\max}/J$.

Boundary conditions. We would like to spend a few words about the boundary conditions at the edges of the computational domain, since they are not standard for moving boundary [16].

At the left edge, we use standard boundary conditions for a wall, namely

$$u = u_w, \quad \frac{\partial p}{\partial x} = 0, \quad \frac{\partial \rho}{\partial x} = 0, \quad (16)$$

where u_w denotes the wall velocity (in our case $u_w = 0$).

The condition on the velocity is obvious, since at the wall the gas has the same velocity of the boundary. The other two conditions can be deduced by a symmetry argument, by considering that a wall is equivalent to having a symmetric gas configuration on the other side of it.

This symmetry consideration no longer applies on the moving boundary, if the speed of the piston is not constant. In this case one has to resort to other conditions. On the moving boundary, the velocity of the gas is equal to piston velocity.

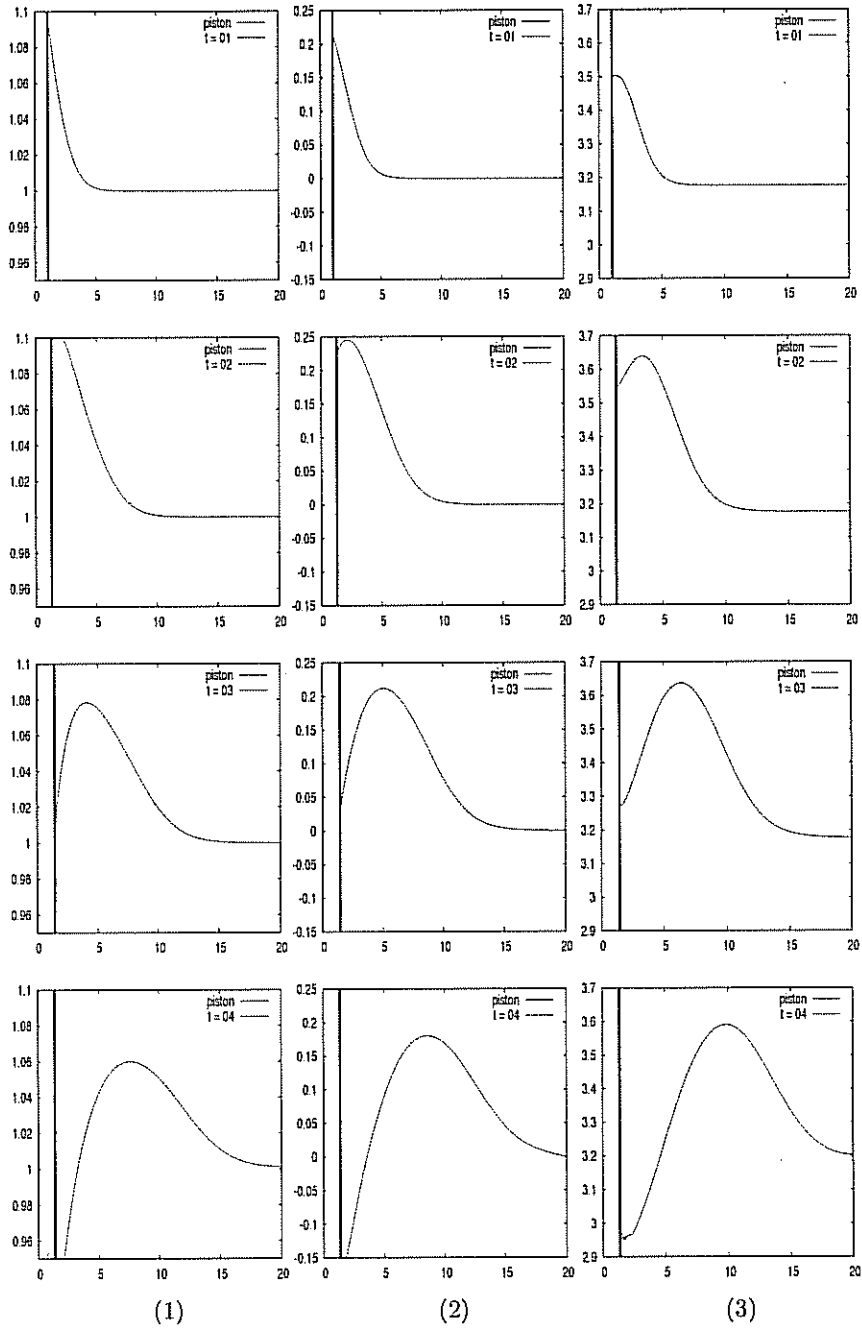


FIGURE 8. Evolution of the moments. $\tau = 10^0$: (1) density ρ , (2) mean velocity u and (3) temperature T at time $t = 1, 2, 3$ and 4 obtained by the semi-Lagrangian method for BGK equations.

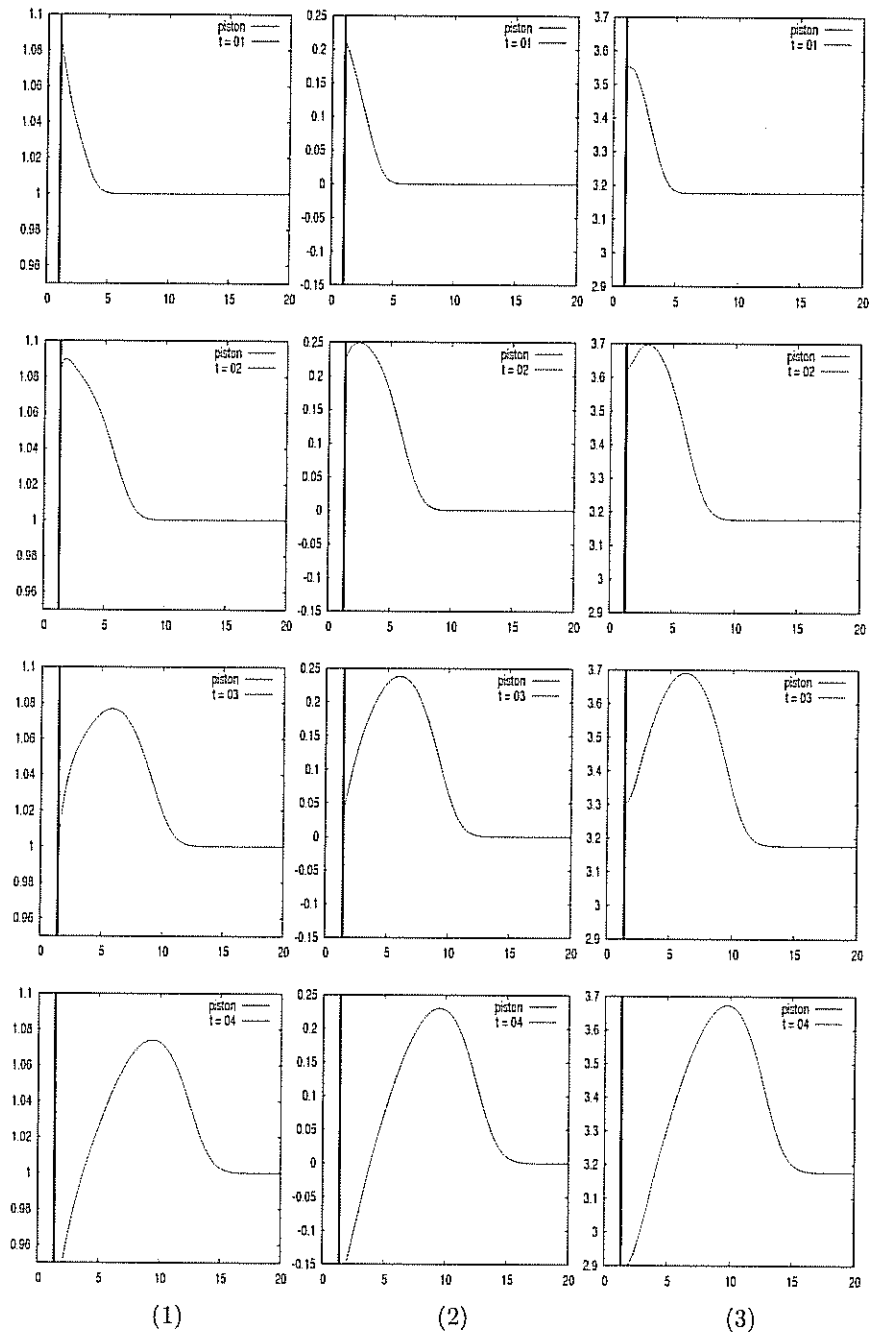


FIGURE 9. $\tau = 10^{-1}$: (1) Density ρ , (2) mean velocity u and (3) temperature T at time $t = 1, 2, 3$ and 4.

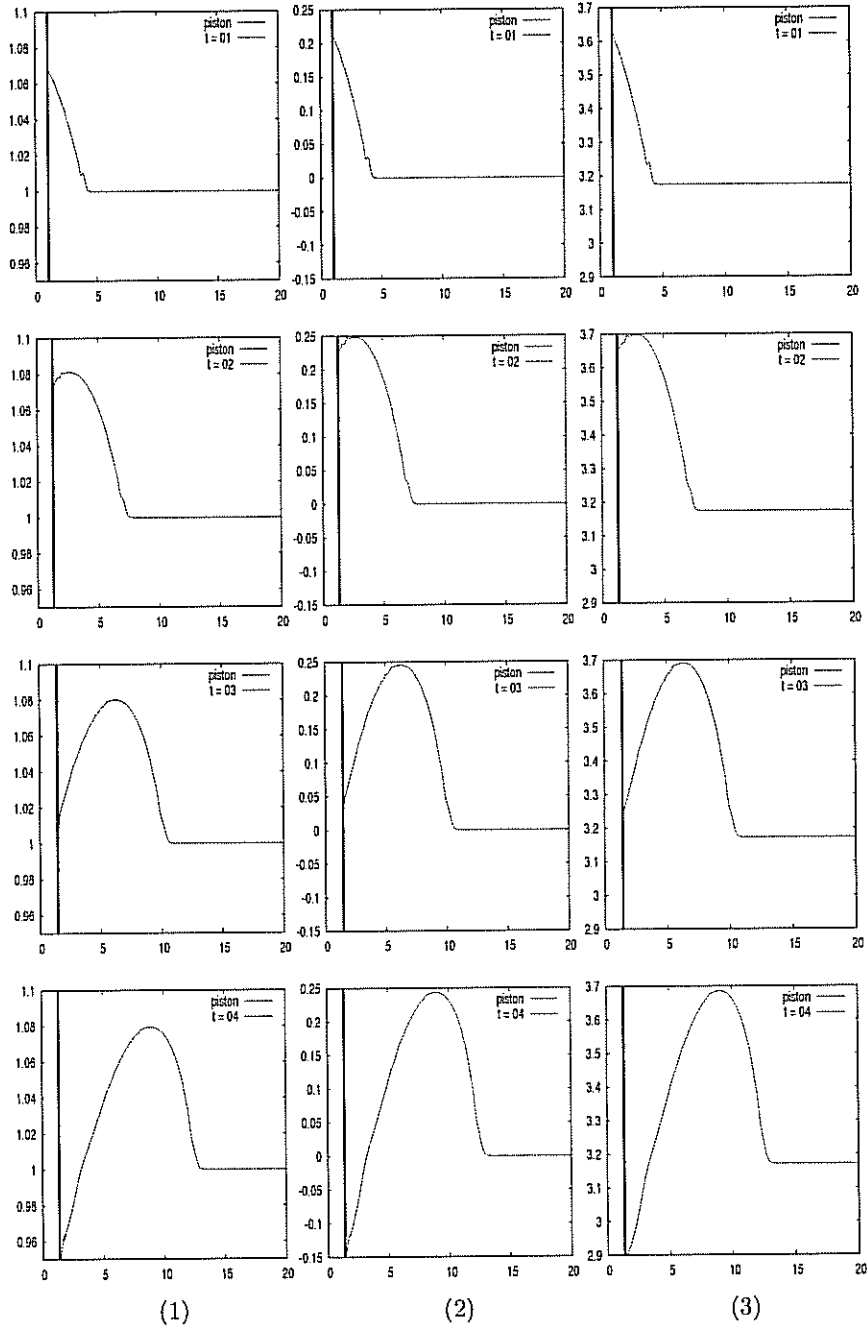


FIGURE 10. $\tau = 10^{-3}$: (1) Density ρ , (2) mean velocity u and (3) temperature T at time $t = 1, 2, 3$ and 4.

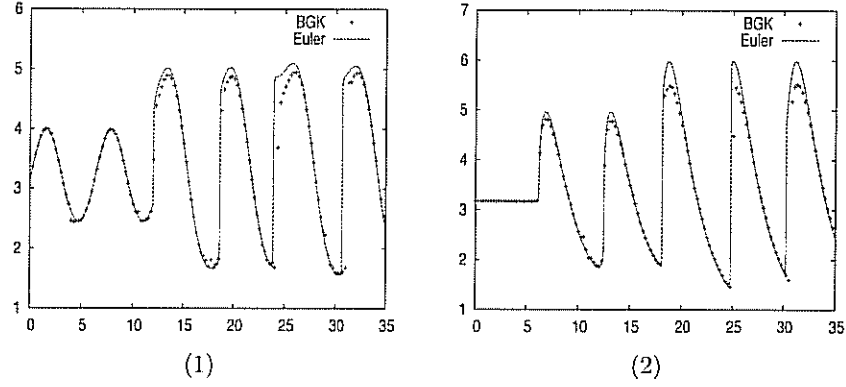


FIGURE 11. $\tau = 10^{-3}$: the pressure at the boundary (1) $x = x_p(t)$ and (2) $x = L$ obtained by the semi-Lagrangian method for BGK equations and a Lagrangian scheme for Euler equations.

Direct compatibility of the boundary condition on the velocity with momentum conservation law, which is

$$\frac{Du}{Dt} + \frac{\partial p}{\partial \xi} = 0,$$

gives

$$\frac{\partial p}{\partial \xi} = -\frac{d^2 x_p(t)}{dt^2}. \quad (17)$$

The condition on the density can be obtained by assuming that, the entropy at the piston is flat, i.e. $\partial S/\partial x = 0$. Note that if such condition is satisfied by the initial condition, it will be maintained by the equations for smooth solutions. This condition, expressed in Eulerian coordinates, becomes

$$\frac{\partial p}{\partial x} = \frac{1}{c_s^2} \frac{\partial p}{\partial x},$$

where $c_s^2 = (\partial p/\partial \rho)_S$ is the square of the sound speed. In Lagrangian coordinates, this relation reads

$$\frac{\partial p}{\partial V} \Big|_S \frac{\partial V}{\partial \xi} = \frac{\partial p}{\partial \xi}, \quad (18)$$

where $-(\partial p/\partial V)_S = \gamma p/V$ is the square of the sound speed in Lagrangian coordinates.

The numerical solution to the gas dynamics equations are obtained by using the second order Nessyahu-Tadmor finite volume central scheme [26] for the system written in Lagrangian coordinates. The boundary conditions for the velocity are obtained imposing that the arithmetic mean of the ghost cell and specularly reflected grid velocity is equal to the piston velocity, while the conditions for pressure and density are obtained from second order discretization of conditions (17-18).

Note that if one discretizes conditions (16) in place of the more accurate (17-18) for the moving boundary, the numerical scheme would still be consistent, but its accuracy would degrade to first order.

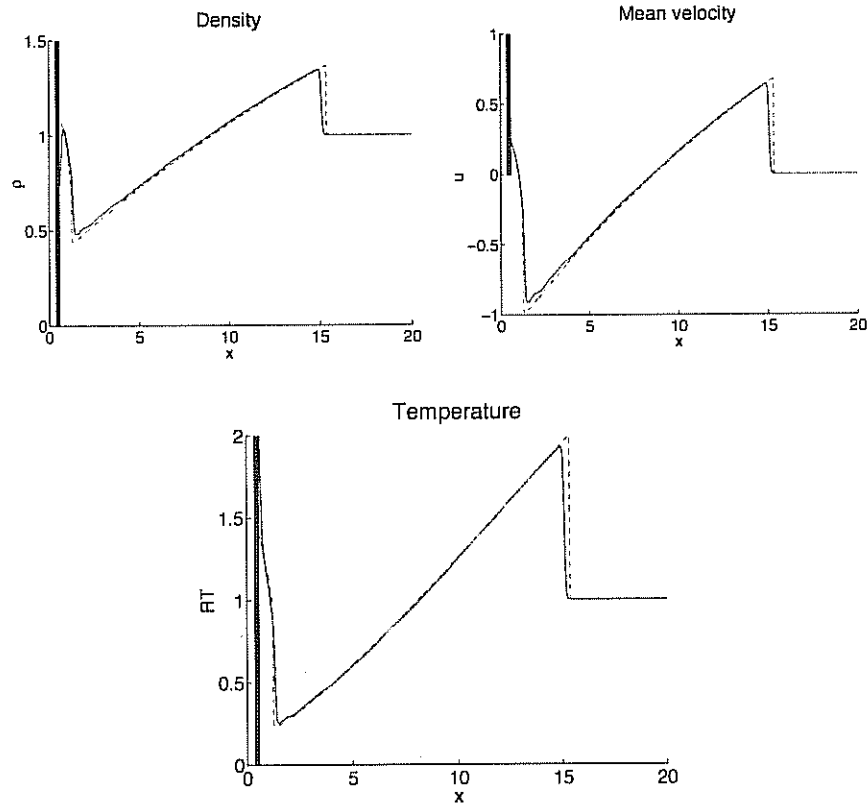


FIGURE 12. Comparison between kinetic and fluid dynamic solutions to the piston problem. Profiles of the density, velocity and temperature at time $t = 5$ for the test problem. The piston is located on the left boundary, and the wall on the right one. Continuous line: BGK solution; dashed line: Euler solution

Conclusions and perspectives. In this paper we introduce a technique for the numerical solution of the BGK equation of rarefied gas dynamics in a domain with moving boundary. The numerical solution is computed on a fixed Cartesian grid, which is a great advantage in terms of simplicity and efficiency. Specular boundary conditions are treated by the use of ghost cells, while diffusive boundary conditions are treated by a more or less standard technique, suitably adapted to the moving boundary. The BGK model has been chosen as a prototype model for the development of the technique, because of its simplicity, and the possibility of capturing the fluid dynamic limit. A comparison with the solution of the Euler equation of gas dynamics for the piston problem shows a very good agreement for the profile of the fields, and for the time dependence of the pressure at the piston and at the wall. The advantages of the present method are the following

- i) because of its Lagrangian nature it allows the use of large CFL numbers,

- ii) the domain can be discretized by a simple Cartesian fixed grid,
- iii) the implicit treatment of the source allows to capture the fluid dynamic limit.

The present scheme is only first order accurate in time, and third order accurate in space. High order in time can be achieved by using the high order Runge-Kutta along the characteristics, as illustrated in [31].

The present work is only a first step in the development of a scheme for the efficient computation of rarefied flows in domains with moving boundaries. The next step is to implement the scheme for two dimensional flows, with three dimensions in velocity, which allows more realistic simulation. A standard approach would require the solution of a distribution function $f(t, x, v)$, with $x \in \mathbb{R}^2$ and $v \in \mathbb{R}^3$. Computer time can be saved by adopting the technique used in [2], where the problem is reduced to the solution of two coupled equations for two functions of (t, x, v) , with $(x, v) \in \mathbb{R}^{2 \times 2}$.

Another natural extension is to consider more realistic Boltzmann collision terms, such as variable hard sphere molecules. Fourier-spectral schemes [29, 18, 19] seem very promising in this direction, for their high accuracy and moderate cost, compared with other deterministic methods. Such methods will be suitable for situations not too far from global equilibrium, where a uniform discretization in velocity will be able to represent the distribution function in the whole domain, and for Knudsen number not too small, where the stiffness in the relaxation is not an issue. In such conditions, high order accuracy in time could be obtained by using Runge-Kutta schemes along characteristics [31].

A convenient way to describe a two-dimensional floating object in a fluid is through the use of level set functions: the boundary of the object is given by the zero level set of a function $\phi(t, x)$, $x \in \mathbb{R}^d$. If the motion of the object is known *a priori*, then the function ϕ is known, and a variant of the method illustrated in this paper can be adopted. If, on the other hand, the motion of the object is not known, and its evolution depends on the interaction with the gas, then the treatment of the problem in the same framework requires some investigation.

Acknowledgments. The authors would like to thank the support received for project MONUMENT (MODellizzazione NUMerica in MEms and NanoTecnologie) by Galileo Programme of the *Università Italo Francese*, institution engaged for the academic cooperation between Italy and France.

REFERENCES

- [1] "Guide to Reference and Standard Atmosphere Models," American Institute of Aeronautics and Astronautics, 1997.
- [2] K. Aoki, K. Kanba and S. Takata, *Numerical analysis of a supersonic rarefied gas flow past a flat plate*, Phys Fluids, **9** (1997), 1144–1161.
- [3] K. Aoki, Y. Sone and T. Yamada, *Numerical Analysis of gas flows condensing on its plane condensed phase on the basis of kinetic theory*, Physics of Fluid A, **2** (1990), 1867–1878.
- [4] P. Andries, P. Le Tallec, J. P. Perlat and B. Perthame, *The Gaussian-BGK model of Boltzmann equation with small Prandtl number* Eur. J. Mech. B Fluids, **19** (2000), 813–830.
- [5] A. Bardow, I. V. Karlin and A. A. Gusev, *General characteristic-based algorithm for off-lattice Boltzmann simulations* Europhys. Lett., **75** (2006), 434–440.
- [6] P. L. Bhatnagar, E. P. Gross and M. Krook, *A model for collision processes in gases. Small amplitude processes in charged and neutral one-component systems*, Physical Reviews, **94** (1954), 511–525.
- [7] G. A. Bird, "Molecular Gas Dynamics and the Direct Simulation of Gas Flows," Clarendon Press, 1995.

- [8] F. Bouchut and B. Perthame, *A BGK model for small Prandtl number in the Navier-Stokes approximation*, J. Stat. Phys., **71** (1993), 191–207.
- [9] E. Carlini, R. Ferretti and G. Russo *A Weighted Essentially Non oscillatory, Large Time-Step Scheme for Hamilton-Jacobi Equations*, SIAM J. Scientific Computing, **27** (2005), 1071–1091.
- [10] J. A. Carrillo and F. Vecil, *Non oscillatory interpolation methods applied to Vlasov-based models*, SIAM J. Sci. Comput., **29** (2007), 1179–1206.
- [11] C. Cercignani “The Boltzmann Equation and its Applications,” Springer, 1988.
- [12] S. Chapman and T. G. Cowling, “The Mathematical Theory of Non-Uniform Gases,” Cambridge University Press, 1970.
- [13] S. Chen, and G. D. Doolen, Lattice Boltzmann method for fluid flows *Annual Review of Fluid Mechanics*, **30** (1998), 329–364.
- [14] F. Coron and B. Perthame, *Numerical passage from kinetic to fluid equation* SIAM J. Numer. Anal., **28** (1991), 26–42.
- [15] P. Degond, J.-G. Liu and M. H. Vignal, *Analysis of an asymptotic preserving scheme for the Euler-Poisson system in the quasineutral limit*, SIAM J. Numer. Anal., **46** (2008), 1298–1322.
- [16] R. Fazio and G. Russo, *A Lagrangian central scheme for interface problems*, preprint.
- [17] F. Filbet and E. Sonnendruker, *Comparison of Eulerian Vlasov solvers*, Comput. Phys. Communications, **150** (2003), 247–266.
- [18] F. Filbet, C. Mouhot and L. Pareschi, *Solving the Boltzmann equation in $N \log N$* , SIAM J. Sci. Comput., **28** (2006), 1029–1053.
- [19] F. Filbet and G. Russo, *High order numerical methods for the space non-homogeneous Boltzmann equation* Journal of Computational Physics, **186** (2003), 457–480.
- [20] A. Frangi, A. Frezzotti and S. Lorenzani, *On the application of the BGK kinetic model to the analysis of gas-structure interactions in MEMS*, Computers and Structures, **85** (2007), 810–817.
- [21] M. Gad-el-Hak, editor, “The MEMS Handbook,” CRC Press, 2002.
- [22] L. H. Holway, “Kinetic Theory of Shock Structure using an Ellipsoidal Distribution Function,” Academic Press, New York, 1966, 193–215.
- [23] S. Jin, *Efficient asymptotic-preserving (AP) schemes for some multiscale kinetic equations*, SIAM J. Sci. Comput., **21** (1999), 441–454 (electronic).
- [24] Axel Klar, *An asymptotic preserving numerical scheme for kinetic equations in the low Mach number limit*, SIAM J. Numer. Anal., **36** (1999), 1507–1527.
- [25] L. Mieussens, *Discrete velocity model and implicit scheme for the BGK equation of rarefied gas dynamics*, Math. Models Methods Appl. Sci., **10** (2000), 1121–1149.
- [26] H. Nessyahu and E. Tadmor, *Non oscillatory central differencing for hyperbolic conservation laws*, J. Comput. Phys., **87** (1990), 408–463.
- [27] L. Pareschi and G. Russo, *Implicit-Explicit Runge-Kutta schemes and applications to hyperbolic systems with relaxation*, J. Sci. Comput., **25** (2005), 129–155.
- [28] L. Pareschi and G. Russo, *An introduction to the numerical analysis of the Boltzmann equation*, Riv. Mat. Univ. Parma, **4**** (2005), 145–250.
- [29] L. Pareschi and G. Russo, *Numerical solution of the Boltzmann equation I: Spectrally accurate approximation of the collision operator*, SIAM J. Numerical Analysis, **37** (2000), 1217–1245.
- [30] S. Pieraccini and G. Puppo, *ImplicitExplicit Schemes for BGK Kinetic Equations* Journal of Scientific Computing, **32** (2007), 1–28.
- [31] P. Santagati, “High Order Semi-Lagrangian Methods for the BGK Model of the Boltzmann Equation,” PhD thesis, University of Catania, 2007.
- [32] O. C. Zienkiewicz and R. Codina, *A general algorithm for compressible and incompressible flow. Part I. The split, characteristic-based scheme* Int. J. Numer. Methods Fluids, **20** (1995), 869–885.

Received November 2008; revised December 2008.

E-mail address: russo@dmf.unict.it

E-mail address: filbet@math.univ-lyon1.fr